Aberystwyth University

Evidence for the tongue of ionization under northward interplanetary magnetic field conditions

Middleton, H. R.; Pryse, Sian; Kersley, Leonard; Bust, G. S.; Fremouw, E. J.; Secan, J. A.; Denig, W. F.

Evidence for the tongue of ionization under northward interplanetary magnetic field conditions

H. R. Middleton,[1] S. E. Pryse,[1] L. Kersley,[1] G. S. Bust,[2] E. J. Fremouw,[3] J. A. Secan,[3] and W. F. Denig[4]

[1] The activities of the International Ionospheric Tomography Community open up new possibilities of simultaneously imaging the large-scale spatial structure of the ionosphere in different longitude sectors. In the study, tomography receiver chains in Scandinavia and Greenland were used to provide a wide view of the plasma density structure in the winter, magnetic postnoon sector under conditions of stable, positive interplanetary magnetic field B_z component. The spatial distributions of the plasma are discussed in light of a high-latitude plasma convection pattern pertinent to the conditions, which is supported by DMSP flow measurements. The observations are consistent with a tongue of dayside photoionization being drawn antisunward by the convection pattern to form an arc of enhanced plasma density around the periphery of the polar cap.

1. Introduction

[2] The morphology of the high-latitude ionosphere is governed by magnetic reconnection between the interplanetary magnetic field (IMF) and the geomagnetic field [*Dungey*, 1961]. The details are dependent upon the strength and orientation of the IMF components. Under conditions of B_z negative reconnection occurs near the equatorial plane, while the anti-parallel geometrical conditions for reconnection of the fields are to be found in the magnetospheric lobes when B_z is positive. Equatorial reconnection drives a two-cell high-latitude convective flow, with antisunward cross-polar flow and return sunward flows at lower latitudes in the dawn and dusk sectors [*Reiff and Burch*, 1985; *Cowley*, 1998]. Lobe reconnection generates a pair of lobe convection cells in the polar cap with sunward flow over the polar cap, which are flanked at lower latitudes by the dawn and dusk convection cells. Tension forces due to the IMF B_y component distort the symmetry of the cells around the noon-midnight meridian [*Cowley et al.*, 1991]. The footprints of the reconnection process are also evident in auroral emissions, with Type 1 and 2 dayside aurora being characteristic of equatorial and lobe reconnection respectively [*Sandholt et al.*, 1998], and in the energy flux of precipitating ions measured by low-altitude satellites [*Newell and Meng*, 1995] as a velocity-filter dispersion effect [*Rosenbauer et al.*, 1975]. More recently, radio tomographic imaging has been used to identify footprints of reconnection in the spatial plasma distribution near local magnetic noon, with plasma on newly opened field lines being drawn poleward under conditions of $B_z < 0$ [*Walker et al.*, 1998], while with $B_z > 0$ dayside plasma is unable to penetrate across the adiaroic boundary into the polar cap [*Pryse et al.*, 2000]. Knowledge of the plasma distribution under different IMF orientations is of direct relevance to the understanding of the large-scale density features that characterise the high-latitude ionosphere, like the tongue of ionization and consequent polar-cap patches [*Weber et al.*, 1986] and arcs [*Carlson et al.*, 1984]. A tongue of photoionization from the dayside has been identified in both modeling [*Sojka et al.*, 1993] and observations [*Valladares et al.*, 1994], entering the cross polar antisunward flow in the polar cap when B_z is negative (southward). A tongue of ionization was also revealed in the dayside polar ionosphere under $B_z < 0$ conditions in a study by *Kersley et al.* [2005]. The study used radio tomography measurements from three different longitude sectors and compared the observations to the spatial distribution of Total Electron Content measured using GPS signals, which has very wide geographic coverage but limited spatial resolution in comparison to the radio tomographic reconstructions. This present paper also presents multichain tomographic observations of a tongue of ionization but under B_z positive (northward). The measurements support the interpretation of a tongue of ionization that is carried toward the polar cap, but is then drawn in an arc round the edge of a polar cap closed to the inflow of plasma under the IMF configuration.

[3] Radio tomography is a technique that has been developed in recent years to produce images of the spatial

---

[1]Institute of Mathematical and Physical Sciences, University of Wales, Aberystwyth, UK.
[2]Applied Research Laboratories, University of Texas at Austin, USA.
[3]NorthWest Research Associates Inc., Bellevue, Washington, USA.
[4]Space Vehicles Directorate, Air Force Research Laboratory, Hanscom AFB, Massachusetts, USA.
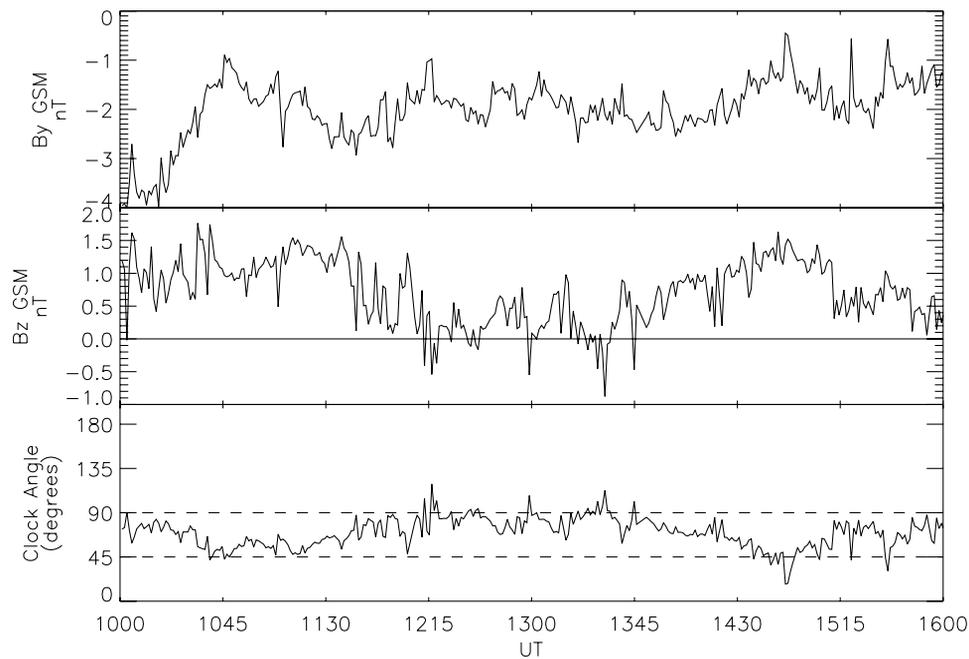
Figure 1. The B_y (top panel) and B_z (middle panel) components of the IMF measured by the ACE satellite in the solar wind between 1000 and 1600 UT on 26 November 2001. The calculated clock angle is shown in the bottom panel with the 45° and 90° levels marked by the dashed lines.

structure of the ionospheric density distribution on horizontal scales of tens to hundreds of kilometres. The fundamentals of the method are described in the review of *Pryse* [2003, and references therein]. In essence, coherent radio transmissions from polar-orbiting satellites are monitored at a chain of receivers on the ground, aligned in longitude but spaced in latitude, to measure the total electron content (TEC) along a large number of intersecting satellite-to-receiver ray paths. Tomographic inversion of the TEC yields an image of the spatial distribution of the electron density in a height-versus-latitude plane of the ionosphere in the region of interest. The International Ionospheric Tomography Community (IITC) has brought together several groups with interests in the field to apply the technique to ionospheric imaging, where routine observations by several chains in different longitude sectors are used to provide information on the plasma distribution over a wide geographic region [*Kersley et al.*, 2005]. The present study employs images from tomography chains in Europe [*Kersley et al.*, 1997] and Greenland [*Coker et al.*, 2001] in a study of the large-scale spatial distribution of the ionospheric plasma in the magnetic postnoon sector in winter, under stable conditions of quiet geomagnetic activity (Kp $\sim$ 1) and positive B_z. To our knowledge this is the first instance in which the distribution of plasma under northward IMF conditions has been imaged over such a large section of the northern polar region.

2. Experimental Observations

2.1. Interplanetary Magnetic Field

[4] The interplanetary magnetic field (IMF), measured upstream in the solar wind by the ACE satellite on 26 November 2001, was stable over an extended period with $B_z > 0$. The B_y and B_z components between 1000 and

1600 UT are shown in the top two panels of Figure 1; B_z was generally positive with $|B_z| \leq 1.5$ nT and B_y negative. The corresponding clock angle (bottom panel) was essentially between 45° and 90° during the time interval. The B_x component (not shown) was relatively constant at about 4 nT after 1015 UT. With the satellite located at approximately $(230, 36, 19)Re$ and a steady solar wind velocity of
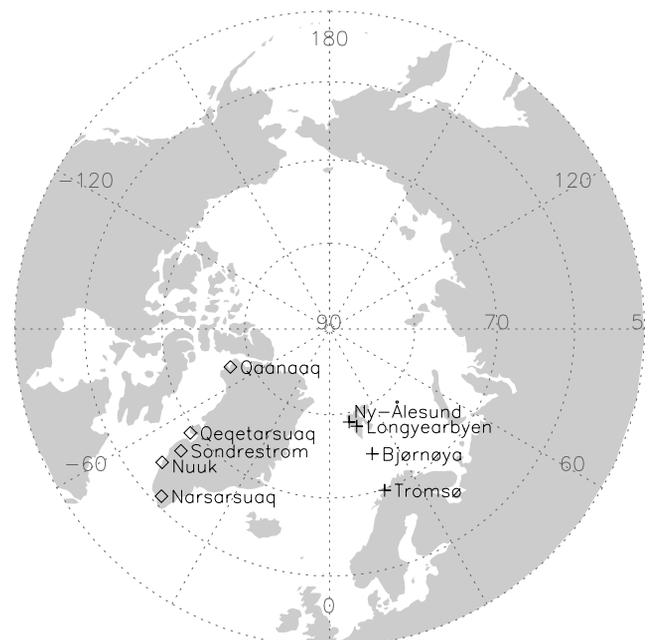

Figure 2. The geographic locations of the receiving stations of the Greenland and Scandinavian tomography chains.
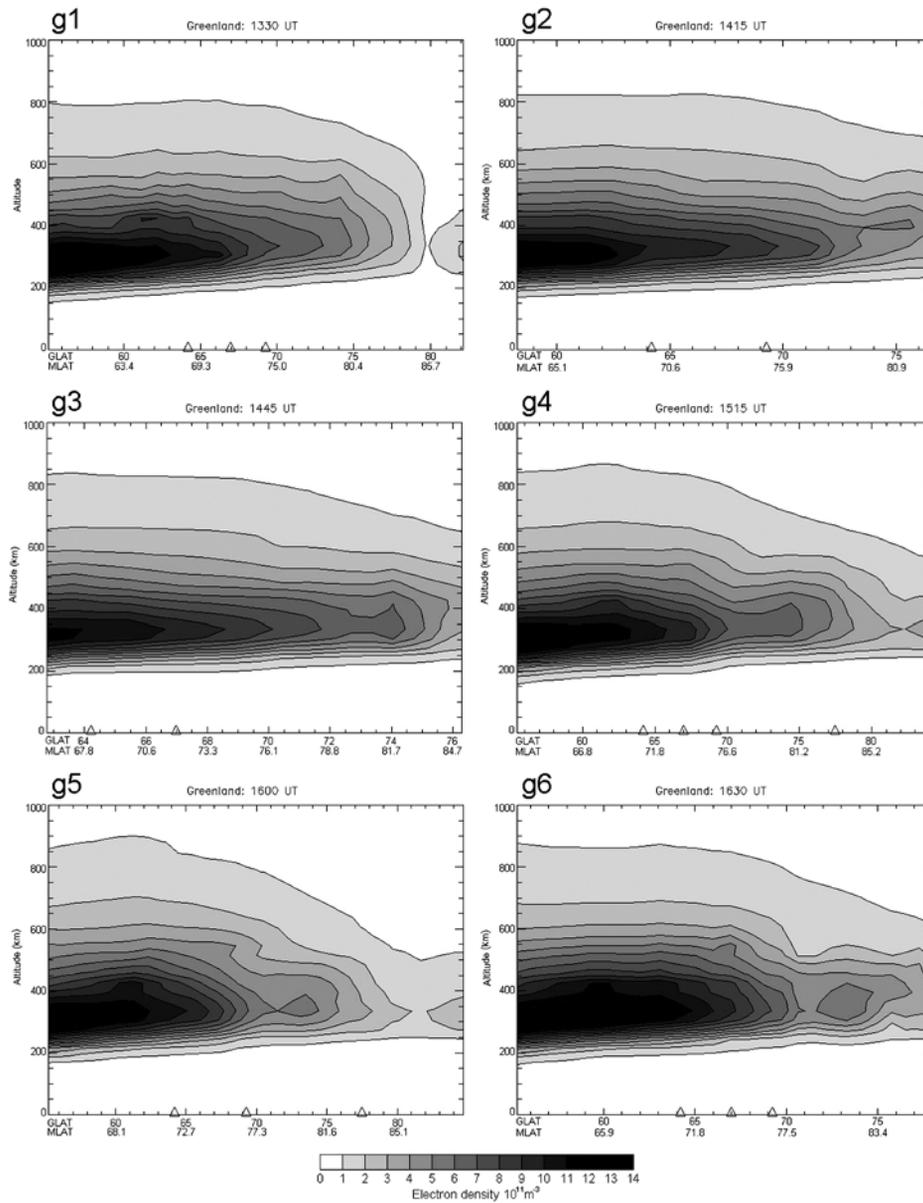
Figure 3. Tomography images from the Greenland chain of the post magnetic noon ionosphere on 26 November 2001. The triangles indicate the geographic locations of the receivers. Note that the *x* axis latitudinal scales are not all the same in all panels.

about 540 km s^{-1}, a simple calculation gives a delay of some 45 min between the measurement in the solar wind and the noontime ionospheric response. Under the prevalent stable conditions, it is not expected that the large-scale ionospheric structure, which is the focus of this study, would have been subject to any significant rapid temporal changes.

2.2. Spatial Distribution of Electron Density

[5] Tomographic observations were made by two receiver chains, one in Greenland and one in Scandinavia (Figure 2), separated by some 70° longitude. Images from the two chains were reconstructed independently for the time period between 1130 and 1630 UT on 26 November 2001. The reconstruction method used for the European chain is described by *Pryse et al.* [1998], and is based on the

Discrete Inverse Theory (DIT) method of *Fremouw et al.* [1994], while that used for the Greenland observations is based on a 3DVAR statistical minimization technique similar to that used in meteorological data assimilation [*Bust et al.*, 2004].

[6] The tomographic reconstructions for the passes monitored at Greenland (g) and Scandinavia (s) are shown in Figures 3 and 4 respectively in terms of geographic and geomagnetic latitudes (GLAT and MLAT respectively) and altitude. The geographic locations of the receiver sites used for each image are shown by the triangles on the latitude axes. All of the reconstructions from the two chains reveal enhanced densities linked to photoionization on the equatorward side of the field-of-view that extend to higher latitudes in the earlier Greenland observations. For the passes monitored later at Greenland and all of the
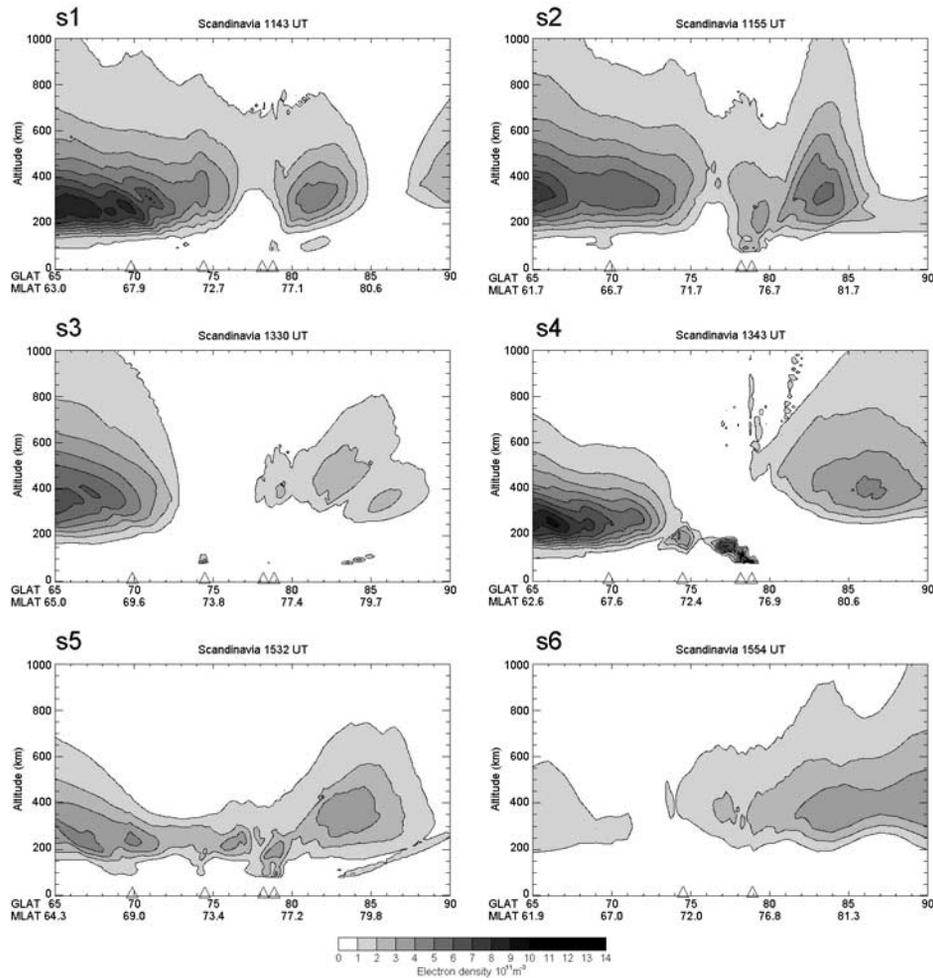
Figure 4. Tomography images from the Scandinavian chain of the post magnetic noon ionosphere on 26 November 2001. The triangles indicate the geographic locations of the receivers.

Scandinavian passes the latitudinal extent of the photoionization is reduced to the north with the densities generally decreasing. Of particular interest to the current study is the ionization at the poleward extreme of the photoionization in the first Greenland pass at 1330 UT. Careful inspection of the panel reveals a discontinuity in the contours with slightly increased densities in the topside near 74°N. The feature can be identified in the following three reconstructions from the Greenland chain, at latitudes between 73°N and 75°N. By the time of the pass at 1600 UT it has become almost detached from the main region of photoionization and is completely separate in the image from the last pass at 1630 UT. The Scandinavian reconstructions also show a blob of ionization that is located between 80°N and 85°N and is separated by a density trough from the region of decaying photoionization at lower latitudes.

[7] To understand this blob structure it is important to view the observations in the geomagnetic reference frame. Figure 5 shows the trajectories of ionospheric intersections at 350 km of the satellite-to-receiver ray paths for each pass on a magnetic latitude versus MLT polar plot. The Greenland passes generally map to the earlier MLTs with those from Scandinavia occurring later in the mag-

netic afternoon. The location of the maximum density of the ionization blob of interest is indicated by the solid circles on individual trajectories and is seen to lie near 80° MLAT. Under the stable prevalent IMF conditions with only small temporal changes, the tomography images can be taken to give the spatial distribution of the postnoon high-latitude ionospheric plasma density. At the earlier MLTs and the ionosphere in sunlight, photoionization can be seen over most of the field-of-view, extending in a continuous tongue of decreasing densities with increasing latitude. However, a density discontinuity can be identified at the poleward extreme of the photoionization, which eventually becomes completely detached at the later MLTs. There is a general decrease in the density level of the detached blob with increasing MLT as the trajectories move into the nightside, with the densities of the last Scandinavian reconstructions being significantly less than the first Greenland reconstructions.

2.3. Plasma Drift

[8] Cross-track horizontal plasma drifts measured during three successive polar passes by the Defense Meteorological Satellite Program (DMSP) F13 spacecraft are plotted in
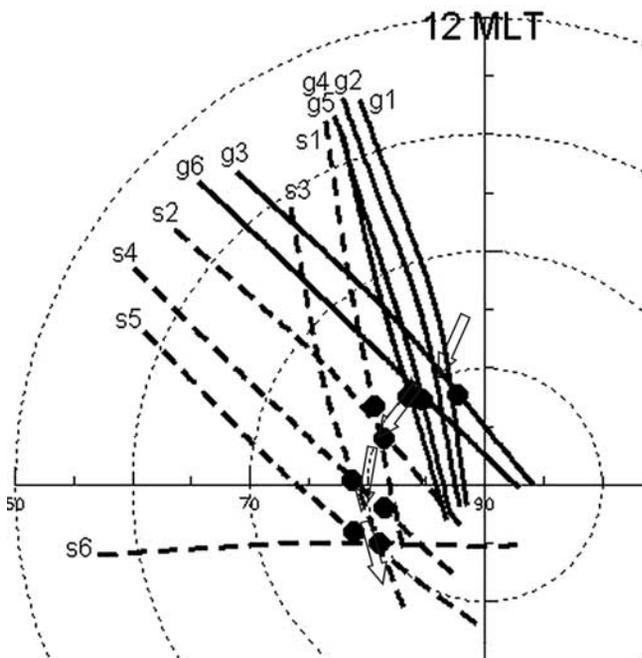
Figure 5. Ionospheric intersections of the satellite-to-receiver ray paths at an altitude of 350 km for the passes monitored in Greenland (g) and Scandinavia (s) as functions of geomagnetic latitude and MLT. The labels match those on the tomographic images in Figures 3 and 4. The solid circles indicate the locations of the ionization blob of interest, and the arrows show the anticipated plasma flow streamline in the post noon sector.

Figure 6. It is important to note that within this magnetic geometry the orbital track for the F13 satellite moved to progressively higher latitudes or, in other words, further away from the dayside and toward the night. These satellite data indicate that high-latitude convection throughout this stable period was dominated by a strong afternoon convection cell consistent with a negative B_y IMF orientation. This particular magnetic geometry also suggests that the convective throat for dayside convection stretched from the late morning sector across local noon and into the postnoon sector at somewhat higher latitudes. Of relevance to this study was the observation in the figure labeled 1143 UT of a clear sunward drift at noon near 82° MLAT. The sunward convection within the polar cap was barely discernable for the higher-latitude pass at 1324 UT and could not be detected in the highest latitude pass at 1505 UT. We surmise from this set of measurements that the dayside sunward drift was indicative of a pair of lobe convection cells that distorted the overall convection pattern near noon within the magnetic latitude range from about 80° to 85° MLAT.

3. Discussion

[9] The spatial distributions of electron density in Figures 3 and 4 can be interpreted in terms of the anticipated high-latitude convection pattern under the conditions of IMF $B_z > 0$ and $B_y < 0$. *Cowley* [1998] indicates that the pattern comprises a pair of lobe cells with a central sunward flow that is displaced to the dawn side and flanked by

viscous cells at dawn and dusk. Under these conditions ionospheric plasma cannot flow in or out of the polar cap across the adiaroic boundary that separates flux tubes of the lobe and viscous cells. The arrows superimposed on Figure 5 near 80° MLAT indicate the plasma flow anticipated on the poleward side of the dusk viscous cell, which have been inferred from the strongest antisunward cross-trajectory flows in top right and bottom of Figure 6 corresponding best in time with the tomography reconstructions. These are taken to represent distorted flow around the polar cap, which is closed to the inflow of plasma. Close inspection of the flows in the two panels of Figure 6 reveals an asymmetrical distribution of the main antisunward velocities with weaker antisunward components persisting to poleward latitudes above ~84° MLAT. These smaller flow components may be representative of antisunward motion in the weaker circulation of the polar duskside lobe cell.

[10] At early MLTs (corresponding to the conditions found in Figure 3, panels g1 and g2) the plasma extends unbroken into the polar latitudes. At these times the satellite trajectories align more or less along plasma flow in the viscous cells that is drawing photoionization antisunward toward the closed polar cap. The photoionization in panel g1 extends northward to a geomagnetic latitude of about 84° MLAT and it is possible that weak photoproduction may even be occurring within the polar lobe cell. However, the plasma blob is clearly seen forming at about 79°–81° MLAT and is thus likely to be in the latitude regime of the stronger antisunward flow component of the viscous cell. This blob is interpreted as convecting photoionization that is unable to penetrate through the adiaroic boundary into the polar cap, and is consequently drawn around the polar region in the flow at the poleward edge of the viscous cell. The trajectories of the image planes at the later MLTs tend increasingly to cut across the flow streamlines, with the tomography reconstructions showing plasma at higher latitudes appearing to detach from the photoionization continuum and become completely separate as the trajectories become more perpendicular to the streamlines. The ionization blob at high-latitudes is interpreted to lie in the antisunward flow at the limit of the viscous cell, with the images showing a cross section through an arc of enhanced ionization that is ringing the periphery of the closed polar cap. Indeed, it can be argued that this enhancement corresponds to the tongue of ionization (TOI) comprising dayside plasma that is initially drawn toward the polar cap in the magnetic noon sector. However, unlike under $B_z < 0$ where the tongue is drawn through the polar cap, it is now not able to cross the adiaroic boundary and access the polar region. It is thus distorted and drawn round the polar cap, possibly both on the dusk and dawn sides, although the present observations cover only the dusk sector. Evidence for a ring of enhanced plasma density round the polar cap with B_z northward has been presented by *Berry* [2000], but it is believed that the current paper is the first to present observations of the TOI when it is unable to enter the polar cap under the $B_z > 0$ IMF configuration.

[11] The tomographic reconstructions from the Greenland chain, shortly after magnetic noon, strongly suggest that the TOI was formed from photoionization being drawn from the sunlit dayside. However, in this instance photoionization is unlikely to be the sole source of the ionization of the
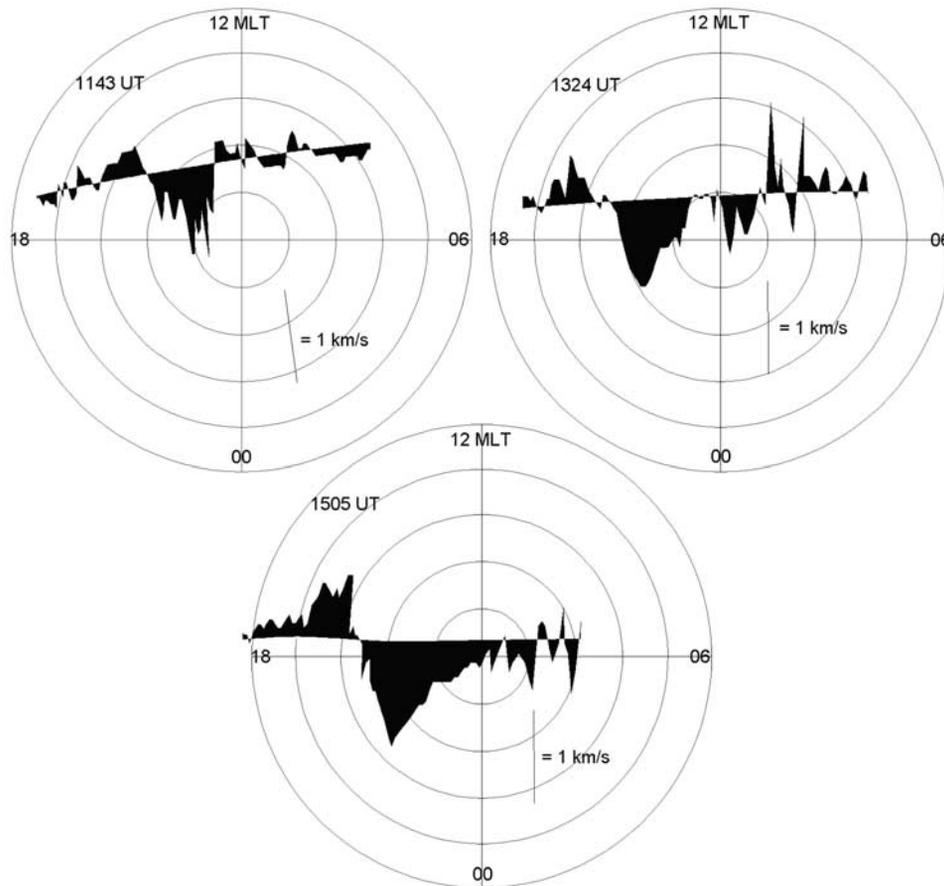
Figure 6. Horizontal cross-trajectory plasma drift measured by the DMSP F13 satellite during three consecutive passes at 1143, 1324 and 1505 UT on 26 November 2001 as a function of MLT and geomagnetic latitude. The geomagnetic latitudes are at 5° intervals from 65° MLAT to 90° MLAT.

tongue. Careful inspection of the density blob in panel s2 of Figure 4 shows its intensification in a region removed from direct sunlight, with its densities being higher than those of s1 panel at a slightly earlier MLT. Such an increase in density may be attributed to ionization production by soft-particle precipitation. Indeed, it can be noted that electron fluxes measured during the earliest DMSP satellite pass at about 1143 UT reveal soft-particle precipitation near-coincident with the blob in panel s2. Hence it is possible that a significant role is played by soft-particle precipitation in modulating and maintaining the density of the TOI at earlier UTs. Away from the immediate postnoon sector the ionization of the extended blob decreases at MLT advances. The lower densities of the blob in panels s3 to s6 of Figure 4 indicate that ongoing soft-particle precipitation cannot be the source of the ionization in this sector, and it can be concluded that the plasma must have originated upstream in the dayside and was transported in the antisunward flow to the locations of observation.

4. Conclusions

[12] Radio tomography observations in northern Europe and Greenland have been used to identify a localised region of enhanced ionization that appears to be drawn round the winter postnoon sector of the polar cap, with the IMF $B_z > 0$. Observations from the tomography chains at two different longitude sectors have been combined to yield the spatial distribution of high-latitude plasma over an extended MLT interval of some 5 hours of UT. The distribution is interpreted in terms of dayside ionization being drawn antisunward toward the polar cap by the high-latitude convection pattern near magnetic noon. With the flux tubes unable to penetrate into the polar region across the adiaroic boundary, the plasma is carried in the antisunward flow at the poleward edge the dusk viscous cell around the closed polar cap, where it gradually decays. It is believed that these observations form the first identification under conditions of positive (northward) IMF of a type of a tongue of photoionization being carried from the dayside around the polar cap. The study also demonstrates the potential of the International Ionospheric Tomography Community to reconstruct and combine images of the high-latitude ionosphere over an extended geographic region.

References

Berry, S. T. (2000), Experimental studies of plasma structuring in the high-latitude ionosphere, Ph.D. thesis, Univ. of Wales, Aberystwyth.

Bust, G. S., T. W. Garner, and T. L. Gaussiran II (2004), Ionospheric Data Assimilation Three Dimensional (IDA3D): A global, multisensor electron density specification algorithm, *J. Geophys. Res.*, *109*, A11312, doi:10.1029/2003JA010234.

Carlson, H. C., V. B. Wickwar, E. J. Weber, J. Buchau, J. G. Moore, and W. Whiting (1984), Plasma characteristics of polar-cap F-layer arcs, *Geophys. Res. Lett.*, *11*, 895–898.

Coker, C., G. Bust, T. L. Gaussiran, J. Waterman, T. Neubert, E. Gudmundsson, and J. Thayer (2001), Tomography in Greenland, paper presented at International Beacon Satellite Symposium, Int. Union of Radio Sci., Boston, Mass.

Cowley, S. W. H. (1998), Excitation of flow in the Earth's magnetosphere-ionosphere system: observations by incoherent scatter radar, in *Polar Cap Boundary Phenomena*, NATO Adv. Stud. Inst. Ser., vol. 509, edited by J. Moen et al., pp. 127–140, Kluwer Acad., Norwell, Mass.

Cowley, S. W. H., J. P. Morelli, and M. Lockwood (1991), Dependence of convective flows and particle precipitation in the high-latitude dayside ionosphere on the X and Y components of the interplanetary magnetic field, *J. Geophys. Res.*, *96*, 5557–5564.

Dungey, J. W. (1961), Interplanetary magnetic field and the auroral zones, *Phys. Rev. Lett.*, *6*, 47–48.

Fremouw, E. J., J. A. Secan, R. M. Bussey, and B. M. Howe (1994), A status report on applying discrete inverse theory to ionospheric tomography, *Int. J. Inf. Syst. Technol.*, *5*, 97–105.

Kersley, L., S. E. Pryse, I. K. Walker, J. A. T. Heaton, C. N. Mitchell, M. J. Williams, and C. A. Willson (1997), Imaging of electron density troughs by tomographic techniques, *Radio Sci.*, *32*, 1607–1621.

Kersley, L., S. E. Pryse, M. H. Denton, G. Bust, E. Fremouw, J. Secan, M. Conde, N. Jakowski, and G. J. Bailey (2005), Radio tomographic imaging of the northern high-latitude ionosphere on a wide geographic scale, *Radio Sci.*, doi:10.1029/2004RS003103, in press.

Newell, P. T., and C.-I. Meng (1995), Cusp low-energy ion cutoffs: A survey and implications for merging, *J. Geophys. Res.*, *100*, 21,943–21,951.

Pryse, S. E. (2003), Radio tomography: A new experimental technique, *Surv. Geophys.*, *24*, 1–38.

Pryse, S. E., L. Kersley, C. N. Mitchell, P. S. J. Spencer, and M. J. Williams (1998), A comparison of reconstruction techniques used in ionospheric tomography, *Radio Sci.*, *33*, 1767–1779.

Pryse, S. E., A. M. Smith, L. Kersley, I. K. Walker, C. N. Mitchell, J. Moen, and R. W. Smith (2000), Multi-instrument probing of the polar ionosphere under steady northward IMF, *Ann. Geophys.*, *18*, 90–98.

Reiff, P. H., and J. L. Burch (1985), IMF B_y-dependent plasma flow and Birkeland currents in the dayside magnetosphere 2. A global model for northward and southward IMF, *J. Geophys. Res.*, *90*, 1595–1609.

Rosenbauer, H., H. Grunwaldt, M. D. Montgomery, G. Paschmann, and N. Skopke (1975), HEOS-2 plasma observations in the distant polar magnetosphere: The plasma mantle, *J. Geophys. Res.*, *80*, 2723–2737.

Sandholt, P. E., C. J. Farrugia, J. Moen, Ø. Noraberg, B. Lybekk, T. Sten, and T. L. Hansen (1998), A classification of dayside auroral forms and activities as a function of IMF orientation, *J. Geophys. Res.*, *103*, 23,325–23,345.

Sojka, J. J., M. D. Bowline, R. W. Schunk, D. T. Decker, C. E. Valladares, R. Sheehan, D. N. Anderson, and R. A. Heelis (1993), Modeling polar-cap F-region patches using time-varying convection, *Geophys. Res. Lett.*, *20*, 1783–1786.

Valladares, C. E., S. Basu, J. Buchau, and E. Friis Christensen (1994), Experimental evidence for the formation and entry of patches into the polar cap, *Radio Sci.*, *29*, 167–194.

Walker, I. K., J. Moen, C. N. Mitchell, L. Kersley, and P. E. Sandholt (1998), Ionospheric effects of magnetopause reconnection observed using ionospheric tomography, *Geophys. Res. Lett.*, *25*, 293–296.

Weber, E. J., J. A. Klobuchar, J. Buchau, H. C. Carlson, R. C. Livingston, O. de la Beaujardiere, M. McCready, J. G. Moore, and G. J. Bishop (1986), Polar cap F-layer patches: Structure and dynamics, *J. Geophys. Res.*, *91*, 2121–2129.

————————————

G. S. Bust, Applied Research Laboratories, University of Texas at Austin, TX 78712, USA.

W. F. Denig, Space Vehicles Directorate, Air Force Research Laboratory, Hanscom AFB, MA 01731, USA.

E. J. Fremouw and J. A. Secan, NorthWest Research Associates Inc., Bellevue, WA 98009, USA.

L. Kersley, H. R. Middleton, and S. E. Pryse, Institute of Mathematical and Physical Sciences, University of Wales, Aberystwyth, SY23 3BZ, UK. (hrm@aber.ac.uk)